

Oxygen Electroreduction on Multi-Walled Carbon Nanotube Supported Metal Phthalocyanines and Porphyrins in Acid Media

Ivar Kruusenberg¹, Leonard Matisen², Kaido Tammeveski^{1,*}

¹Institute of Chemistry, University of Tartu, Ravila 14a, 50411 Tartu, Estonia

²Institute of Physics, University of Tartu, Riia 142, 51014 Tartu, Estonia

*E-mail: kaido.tammeveski@ut.ee

Received: 15 November 2012 / Accepted: 10 December 2012 / Published: 1 January 2013

Metal phthalocyanine and porphyrin functionalized multi-walled carbon nanotubes (MWCNTs) were used as non-precious electrocatalysts for the electroreduction of oxygen. The catalyst materials were heat-treated at different temperatures before electrochemical testing. X-ray photoelectron spectroscopic study was carried out in order to examine the surface composition. The oxygen reduction reaction (ORR) has been investigated on Fe phthalocyanine/MWCNT, Co phthalocyanine/MWCNT, Fe porphyrin/MWCNT and Co porphyrin/MWCNT catalysts. Electrochemical experiments were carried out in 0.5 M H₂SO₄ solution employing the rotating disk electrode (RDE) method. The RDE measurements showed increase of electrocatalytic activity for MN₄ macrocycle/MWCNT modified electrodes in acid media and catalytic activity increased with increase of pyrolysis temperature. Particularly high electrocatalytic activity for ORR was observed for electrodes heat-treated at 800 °C. The RDE results obtained indicate the effect of different nitrogen groups introduced by pyrolysis on the electrocatalytic activity.

Keywords: Oxygen reduction; Electrocatalysis; Carbon nanotubes; Porphyrin; Phthalocyanine

1. INTRODUCTION

In order to reduce the high price of proton-exchange membrane fuel cells (PEMFCs), Pt-based cathode catalysts need to be replaced with cheaper alternatives. Novel PEMFC catalysts must overcome a number of kinetic limitations on the oxygen reduction reaction (ORR). To eliminate these limitations stable cathode catalysts with an order of magnitude increase in the specific activity over that of state-of-the-art carbon-supported platinum (Pt/C) catalyst can be developed [1,2]. Numerous fundamental and practical approaches have been made to improve electrocatalytic performance and stability of high surface area carbon supports for metal nanoparticle based catalyst materials [3-5].

Catalyst support materials exhibit major influence on the performance and durability of proton exchange membrane fuel cells [6]. Due to their excellent mechanical and chemical properties carbon nanotubes can serve as stable support for metal nanoparticle-based catalyst materials [7-8]. With different possibilities of their large-scale synthesis, attention is now being focused on their potential applications in various fields of heterogeneous catalysis. A number of methods have been used to disperse and stabilize metal nanoparticle-carbon nanotube composite materials. Catalytic properties of these solids are known to be dependent upon the interaction between the carbon support and the metal particles. By meeting the requirements for highly-durable fuel-cell operation multi-walled carbon nanotubes (MWCNTs) turned out to be a promising potential support for ORR catalysts [9,10].

Among the noble and non-noble metal catalysts, the transition metal-nitrogen containing MN_4 macrocycles have achieved huge interest because of their high electrocatalytic activity toward oxygen reduction and competitive price on the market. Starting from the pioneering work of Jasinski [11], the ability of MN_4 macrocycles to reduce O_2 has led to an enormous research activity of these materials in the field of oxygen reduction electrocatalysis both in alkaline and acid media [12-18]. There is a general agreement in the literature that both nitrogen ligands and transition metal in MN_4 macrocycle catalysts play an important role in their stability and activity, even if the constituents of the final active sites are uncertain [19,20]. Phthalocyanines and porphyrins containing iron or cobalt as a central metal atom are one of the most commonly studied and also one of the most promising MN_4 macrocycle electrocatalysts for O_2 reduction, especially when they are adsorbed on the surface of high-area carbons such as carbon nanotubes [21-29]. MN_4 macrocycles form bulky particles during the pyrolysis because of the melting of the porphyrins and phthalocyanines previous to their polymerization [30]. In such kind of catalyst material only a small number of the active sites can participate in the oxygen reduction reaction because of the low surface area. Therefore it has been demonstrated that the type of support to which the phthalocyanine or porphyrin is attached to, also has a significant effect on the electrocatalytic activity [30,31]. It is important to keep in mind that the morphology of the catalyst material and surface area will influence strongly the electrocatalytic activity for the oxygen reduction reaction. MWCNTs with their large surface area and well-defined structure are perfect support material from this point of view. Therefore the aim of the present study is to show the potential of carbon nanotubes as a support for metal macrocyclic catalysts.

A number of studies have shown that heat-treatment of MN_4 macrocycles in an inert atmosphere at high temperatures significantly improved the O_2 reduction activity and stability of these catalyst materials. Since the pioneer study of Jahnke et al. who reported the effect of heat-treatment, numerous research efforts have been made to find and optimize the perfect parameters of the pyrolysis as well to clarify the exact structure of the catalytic center causing the electrocatalytic activity toward the ORR. In the latter case it was found that the transition metal of the precursor is bonded via nitrogen to a graphite-like carbon matrix which was formed by the pyrolysis reaction. It has been proposed that the inner core structure of the MN_4 macrocycle remains after the pyrolysis and acts as a catalytic center for ORR [30].

The purpose of this work is to study and compare the electrocatalytic activity of multi-walled carbon nanotubes modified with different porphyrins and phthalocyanines for the oxygen reduction reaction in acid media. Our goal is to show difference of porphyrins and phthalocyanines from ORR

catalyst point of view and to find optimum pyrolyzing conditions in order to achieve a higher activity and stability of the catalysts studied.

2. EXPERIMENTAL

2.1. Materials

The iron(II)phthalocyanine (FePc), cobalt(II)phthalocyanine (CoPc), 5,10,15,20-tetrakis(4-methoxyphenyl)-21H,23H-porphine cobalt (II) (CoPh) and 5,10,15,20-tetrakis(4-methoxyphenyl)-21H,23H-porphine iron (II) chloride (FePh) were purchased from Sigma-Aldrich. The multi-walled carbon nanotubes (MWCNTs, purity > 95%, diameter 30 ± 10 nm, length 5-20 μm) used were purchased from NanoLab, Inc. (Brighton, MA, USA). 5 wt.% Nafion solution (Aldrich) was used in the preparation of catalyst ink in isopropanol. All the solutions were prepared with Milli-Q water (Millipore, Inc.).

2.2. Preparation of FePc/MWCNT, CoPc/MWCNT, FePh/MWCNT and CoPh/MWCNT catalysts

In order to adsorb the metal macrocyclic catalyst on the surface of MWCNTs, a mixture of 200 mg FePc, CoPc, FePh or CoPh and 200 mg of MWCNTs in 40 ml isopropanol was prepared and sonicated for 30 min followed by magnetic stirring for 1 h. The homogeneous mass was placed in a ceramic boat, dried at 100 °C and pyrolyzed at 400 °C or 800 °C for 2 h in flowing argon atmosphere. The initial loading of FePc, CoPc, FePh or CoPh on the MWCNTs was 50 wt.% and the final loading was not ascertained.

2.3. X-ray photoelectron spectroscopy analysis

The surface composition of the as-received MWCNT and pyrolyzed FePc/MWCNT, CoPc/MWCNT, FePh/MWCNT and CoPh/MWCNT materials was analyzed using X-ray photoelectron spectroscopy (XPS). For the XPS studies the catalyst materials in isopropanol (1 mg ml^{-1}) were deposited on a glassy carbon plate ($1.1 \times 1.1 \text{ cm}$) and the solvent was allowed to evaporate in air. The XPS measurements were carried out with a SCIENTA SES-100 spectrometer using an unmonochromated Mg K α X-ray source (incident energy = 1253.6 eV), a take-off angle of 90 degrees and a source power of 300 W. The pressure in the analysis chamber was below 10^{-9} Torr. While collecting the survey scan, the following parameters were used: energy range = 800 to 0 eV, pass energy = 200 eV, step size = 0.5 eV and for the high resolution scan: energy range = 410 to 395 eV for the N1s region; 740 to 700 eV and 800 to 775 eV for the Fe2p and Co2p regions, respectively, with pass energy = 200 eV and step size = 0.1 eV.

2.4. Preparation of electrodes and electrochemical characterization

For the rotating disk electrode (RDE) experiments a glassy carbon (GC) disk of geometric area (A) of 0.2 cm^2 was used as substrate material. GC disks (GC-20SS, Tokai Carbon) were pressed into a Teflon holder and then the electrodes were polished to a mirror finish with 1 and $0.3 \mu\text{m}$ alumina slurries (Buehler). After alumina polishing the electrodes were sonicated in water for 5 min. To obtain a uniform layer of electrocatalyst onto GC surface, the electrodes were modified with different catalysts using suspensions of MPc/MWCNT or MPh/MWCNT in isopropanol (1 mg ml^{-1}) containing 0.5% Nafion solution. All the suspensions were sonicated for 1 h. Then a $20 \mu\text{l}$ aliquot of the prepared catalyst suspension was pipetted onto GC surface and was allowed to dry in air for 24 h.

The electrochemical measurements were made using the RDE technique employing an EDI101 rotator and a CTV101 speed control unit (Radiometer). Experiments were controlled with the General Purpose Electrochemical System (GPES) software and the potential was applied with an Autolab potentiostat/galvanostat PGSTAT30 (Eco Chemie B.V., The Netherlands). A Pt foil served as the counter electrode and a saturated calomel electrode (SCE) was used as a reference. All the potentials are referred to this electrode. Electrochemical experiments were carried out in $0.5 \text{ M H}_2\text{SO}_4$ solution at room temperature ($23 \pm 1 \text{ }^\circ\text{C}$). The solutions were saturated with Ar (99.999%, AGA) or O_2 (99.999%, AGA). A continuous flow of gases was maintained over the solution during the electrochemical measurements.

3. RESULTS AND DISCUSSION

3.1. XPS analysis of metal phthalocyanine and porphyrin modified MWCNT samples

The X-ray photoelectron spectroscopy (XPS) was used to study the surface composition of the electrocatalysts and to determine the chemical states of species on the surface. Figure 1a and 1b presents the XPS survey spectra of heat-treated CoPh/MWCNT and CoPc/MWCNT samples, respectively. All the samples were heat-treated at $800 \text{ }^\circ\text{C}$. It is possible to separate five similar XPS peaks for both samples, which correspond to emission from C1s, satellite peak of the C1s spectrum, N1s, O1s, and Co2p levels. The XPS core-level spectrum in the N1s region of CoPc/MWCNT and CoPh/MWCNT samples shows two peaks. The N1s peak of higher binding energy at 400.2 eV corresponds to a new nitrogen species formed likely during the pyrolysis and the peak at 399.8 eV could be assigned to N introduced into the graphene layer but it is hard to define the exact chemical nature of these surface species and the identification of the species is still under debate. Two similar nitrogen peaks to CoPc/MWCNT and CoPh/MWCNT samples have been observed also for ClFeTPP on acetylene black and in this case they were assigned to C-N-Hx and C-N-M groups evolved from the decomposition of the MN_4 chelates [32].

The O1s peak is related to the MWCNT material and is caused by various carbon-oxygen functionalities on the surface of MWCNTs [33]. Similarly to the N1s peak, it is hard to define the exact chemical nature of different surface species from O1s peak because of close binding energies and

the topic is still under debate, but different investigations have shown that carboxyl and quinone groups are present on the surface of carbon nanotubes [34].

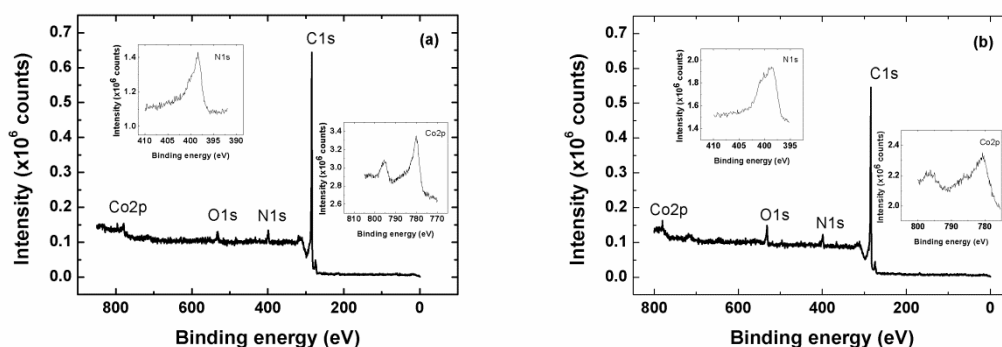


Figure 1. XPS spectra of the catalyst materials (a) CoPh/MWCNT and (b) CoPc/MWCNT with inset spectra of N1s and Co2p.

From the inset of Figures 1a and 1b one can observe XPS peaks at peak at 795.8 eV which corresponding to $\text{Co}2p_{3/2}$ lower energy and 780.2 eV corresponding to $\text{Co}2p_{1/2}$ higher energy asymmetric bands originating from spin-orbital splitting. The peak at 780.2 eV belongs to Co^{2+} from all CoPc/MWCNT or CoPh/MWCNT respectively. The XPS peak at 778.5 eV corresponds to metallic cobalt and peak at 781 eV corresponding to pure CoPc or CoPh respectively. It should be noted that nitrogen or metal catalyst impurities were not detected in the as-received MWCNT samples by XPS.

3.2. Rotating disk electrode studies of O_2 reduction

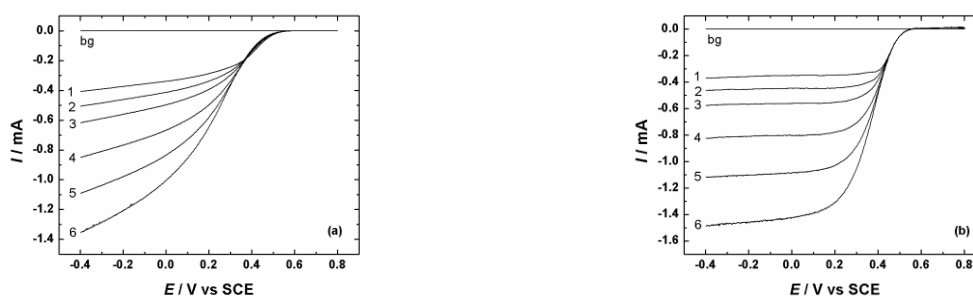


Figure 2. RDE voltammetry curves for oxygen reduction on (a) FePh/MWCNT and (b) CoPh/MWCNT modified GC electrodes in O_2 saturated 0.5 M H_2SO_4 . $\nu = 10 \text{ mV s}^{-1}$. $\omega =$ (1) 360, (2) 610, (3) 960, (4) 1900, (5) 3100 and (6) 4600 rpm.

Typical RDE polarization curves obtained for different MN_4/MWCNT modified electrodes toward ORR in acid media is illustrated in Figure 2a and 2b. The Figures present the RDE results of oxygen electroreduction obtained with FePh/MWCNT and CoPh/MWCNT materials pyrolyzed at 800

°C. The experiments were performed at different rotating rates in O₂-saturated 0.5 M H₂SO₄ solution. An almost constant onset potential of the ORR on the same catalyst at different rotation rates shows that no catalyst material have left from the electrode and no changes are taking place with catalyst material during the experiment. As expected, the limiting currents in a hydrodynamic experiment increase with increasing rotation rate.

To compare these two materials with each other, it is possible to see from Figure 2 that the value of onset potential is similar for both materials, but the difference in half-wave potential is almost 0.2 V. Also the current plateau is formed at a much more positive potential for the CoPh/MWCNT catalyst. Still both of the catalysts increase remarkably the ORR activity. For the heat-treated FePh/MWCNT and CoPh/MWCNT catalysts a high reduction current was observed probably because of the generation of electrocatalytically active species which usually form during the heat-treatment at temperatures higher than 650 °C [16,35]. Ladouceur et al. reported that the electrocatalytic activity of CoPc/Vulcan XC-72, which was annealed at 800 °C, was twice as high as the activity of the non-pyrolyzed CoPc/Vulcan XC-72 [36]. It has been proposed that the electrocatalytically active sites for ORR could be the central metal ion with N atoms [37]. Even if the metal nanoparticles on carbon supports are sometimes reported not to be related to the activity of the catalyst and nitrogen not being a part of the catalytically active site for ORR, these two species together can form highly active catalyst center for ORR [37].

The number of electrons transferred per O₂ molecule (*n*) was calculated from the Koutecky-Levich (K-L) equation [38]:

$$\frac{1}{I} = \frac{1}{I_k} + \frac{1}{I_d} = -\frac{1}{nFAkC_{O_2}^b} - \frac{1}{0.62nFAD_{O_2}^{2/3}\nu^{-1/6}C_{O_2}^b\omega^{1/2}} \quad (1)$$

where *I* is the measured current, *I_k* and *I_d* are the kinetic and diffusion limited currents, respectively; *k* is the electrochemical rate constant for O₂ reduction, *D_{O₂}* is the diffusion coefficient of oxygen (*D_{O₂}* = 1.8×10⁻⁵ cm² s⁻¹ [39]), *c_{O₂}^b* is its concentration in the bulk (*c_{O₂}^b* = 1.13×10⁻⁶ mol cm⁻³ [39]) and *ν* is the kinematic viscosity of the solution (0.01 cm² s⁻¹).

Figure 3a and 3b presents the K-L plots obtained from the RDE data on oxygen reduction in 0.5 M H₂SO₄ for annealed FePh/MWCNT and CoPh/MWCNT catalyst modified electrodes, respectively. The extrapolated K-L lines showed non-zero intercepts, indicating that the process of oxygen reduction is under the mixed kinetic-diffusion control in a large range of potentials. The values of *n* at different potentials are presented as insets in Figure 3a and 3b for FePh/MWCNT and CoPh/MWCNT, respectively.

For both the FePc/MWCNT and CoPh/MWCNT materials the *n* value was close to 3 for all over the range of potential. This indicates that the mixed 2e⁻ and 4e⁻ process takes place and the reduction of O₂ produces both H₂O₂ and H₂O.

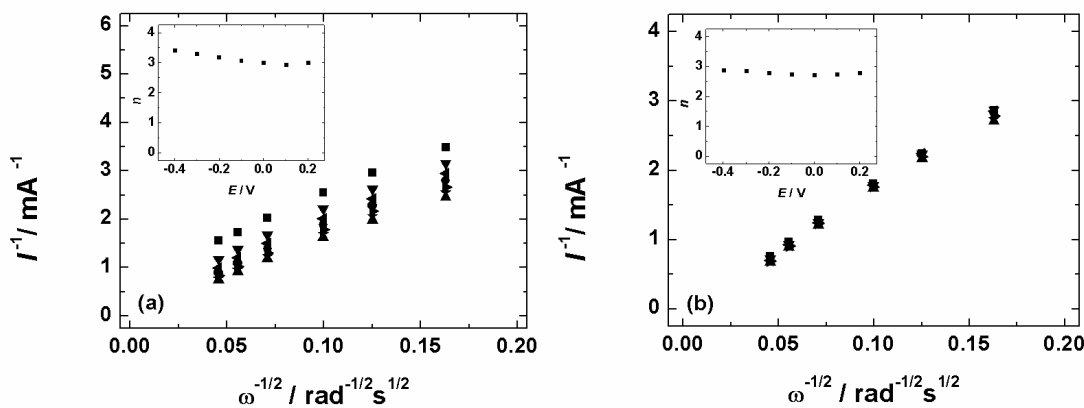


Figure 3. Koutecky-Levich plots for oxygen reduction on (a) FePh/MWCNT and (b) CoPh/MWCNT modified GC electrodes in O_2 saturated 0.5 M H_2SO_4 at various potentials: (■) 0.2, (▼) 0.1, (◄) 0, (●) -0.1, (►) -0.2, (★) -0.3 and (▲) -0.4 V. The inset shows the potential dependence of n .

Figure 4 presents the comparative RDE results of O_2 reduction obtained for GC electrodes modified with different MWCNT supported MN_4 macrocyclic catalyst materials annealed at different temperatures. For comparison purposes the RDE voltammetry curve of unmodified MWCNTs has been added. For each catalyst material the polarization curves of oxygen reduction are presented for unannealed catalyst and materials pyrolyzed at 400 °C and 800 °C. As presented in Figure 4, the electrocatalytic activity for ORR of metallo-porphyrin/MWCNT-GC electrodes was higher than that of the metallo-phthalocyanine/MWCNT modified electrodes. Especially higher activity was observed for CoPh/MWCNT material for which the onset potential of O_2 reduction shifted positive for almost 0.1 V as compared to that of FePc/MWCNT which was the catalyst with poorest ORR activity. As expected, the catalytic activity of all metallo-phthalocyanine and metallo-porphyrin modified MWCNT catalysts improved enormously comparing to pristine MWCNTs. It is well-known that pure MWCNTs itself have rather low electrocatalytic activity for O_2 reduction in acid media [33]. One can see that the onset potential of O_2 reduction on unmodified MWCNTs is substantially more negative than that of metallo-phthalocyanine and metallo-porphyrin modified MWCNTs. This indicates that the catalyst activity is entirely determined by the catalytically active sites formed by the attachment of MN_4 macrocycles to the surface of MWCNTs.

We could expect similar performance for analogous catalysts to large conjugated organometallic molecules as phthalocyanines and porphyrins which easily adsorb on MWCNT support. However there are visible differences in catalytic activity between these materials, which could be explained by the existence of better π - π interactions between MN_4 macrocycle and MWCNTs and by small differences in the structure of the molecules [40,41]. Given the results of the polarization curves for different materials annealed at two different temperatures it can be concluded that the samples heat-treated at 800 °C showed the best electrocatalytic activity toward the ORR. It has been proposed that pyridinic-type nitrogen, forming at temperatures as high as 800 °C, could be responsible for the achieved catalytic activity [42].

It is proven that annealing temperature will enhance the kinetic current density of the catalyst materials and reduce the concentration of MN_4 macrocycles in the pyrolysis product. Gupta et al. stated that the presence of MN_4 macrocycles was not important for the ORR activity in acid media without any annealing [43].

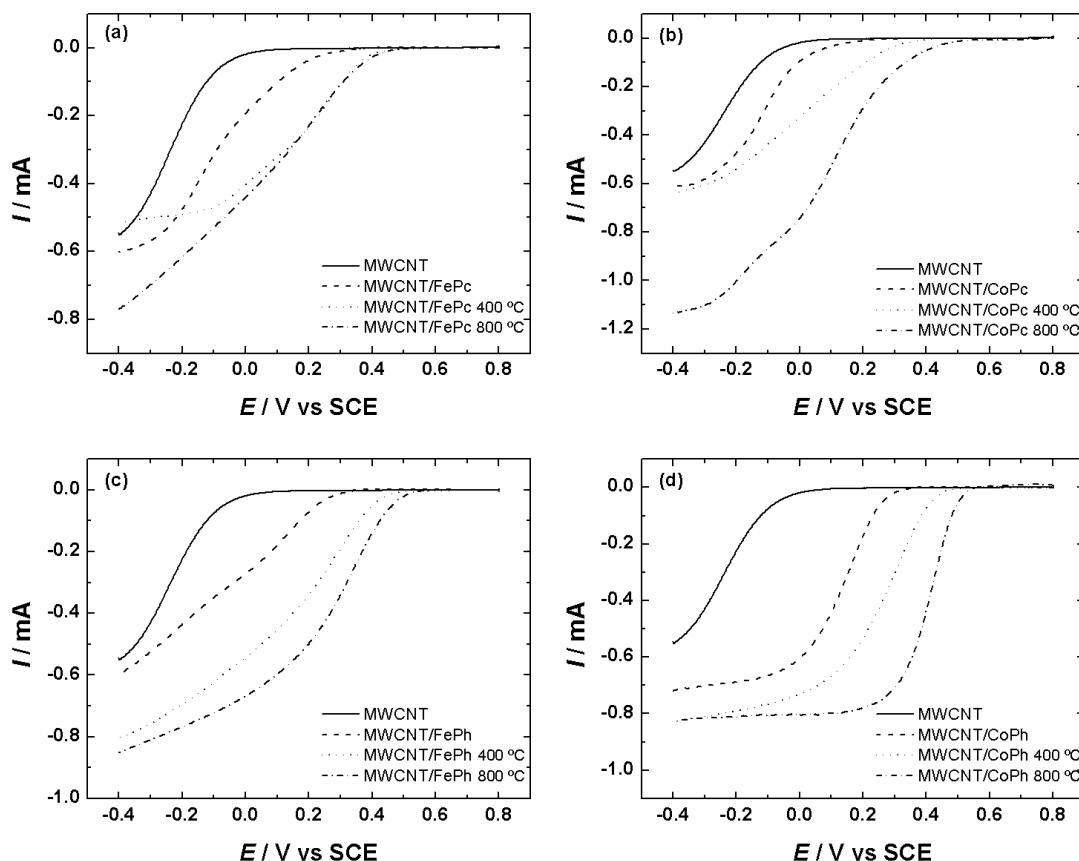


Figure 4. RDE voltammetry curves for oxygen reduction on (a) FePc/MWCNT, (b) CoPc/MWCNT, (c) FePh/MWCNT and (d) CoPh/MWCNT catalyst material modified GC electrodes in O_2 saturated $0.5\text{ M H}_2\text{SO}_4$. $\nu = 10\text{ mV s}^{-1}$. $\omega = 1900\text{ rpm}$.

However comprehension of the exact mechanism and participation of MN_4 -centers in the oxygen reduction mechanism is still discussed controversially [44-46]. From one side MN_4 -centers is believed to be responsible for the improved catalytic effect, from another hand nitrogen heteroatoms are favored as catalytic sites [47-49]. It is proven that when nitrogen is presented in the carbon matrix, the ORR proceeds only at low current densities, high overpotentials and therefore produces hydrogen peroxide [48,50]. Still the nitrogen plays important role in the MN_4 catalyst material and has been proved by Lalande et al. who achieved highest catalytic activity with complex material having both nitrogen and metal presented [51]. Therefore metal- N_4^- or metal- N_{2+2} are suggested as active sites [47].

Some research groups have also suggested that quinone groups presented on the surface of carbon materials could take part from the formation of active sites. Elbaz et al. presented evidences about the formation of stabilized MN_4 macrocycle-quinone complexes at carbon-based surfaces toward design of non-noble-metal catalyst for the oxygen reduction reaction [51].

4. CONCLUSIONS

Non-noble metal electrocatalysts namely Co phthalocyanine, Fe phthalocyanine, Co porphyrin and Fe porphyrin were adsorbed on the surface of multi-walled carbon nanotubes. All of these catalyst materials were heat-treated at 400 °C and 800 °C in an inert atmosphere. The surface composition of MWCNT supported Co and Fe phthalocyanines and porphyrins were examined by XPS. The XPS results showed decomposition of the porphyrin ring because of the pyrolysis and the formation of different electrocatalytically active metallic and nitrogen surface groups. These electrocatalysts were also examined toward the ORR kinetics by RDE method in 0.5 M H₂SO₄ and it was found that metal-porphyrin based electrodes heat-treated at 800 °C possessed higher O₂ reduction activity compared with metal-phthalocyanine catalysts. The results obtained in the present work further highlight the advantages of carbon nanotube supported MN₄ macrocycles as electrocatalysts for ORR [52].

ACKNOWLEDGEMENT

This research was supported by the Estonian Science Foundation (Grant No. 9323).

References

1. D.S. Cameron, *Platinum Metals Rev.*, 55 (2011) 108.
2. B. Wu, M. Matian and G.J. Offer, *Int. J. Low Carbon Technol.*, 7 (2012) 28.
3. F. Memioglu, A. Bayrakçeken, T. Öznülüer and M. Ak, *Int. J. Hydrogen Energy*, 37 (2012) 16673.
4. M.S. Ahmed and S. Jeon, *J. Power Sources*, 218 (2012) 168.
5. J. Liu, L. Lai, N.G. Sahoo, W. Zhou, Z. Shen and S.H. Chan, *Aust. J. Chem.*, 65 (2012) 1213.
6. W. Zhang, P. Sherrell, A.I. Minett, J.M. Razal and J. Chen, *Energy Environ. Sci.*, 3 (2010) 1286.
7. W.M. Daoush and T. Imae, *J. Mater. Res.*, 27 (2012) 1680.
8. B.P. Vinayan, R.I. Jafri, R. Nagar, N. Rajalakshmi, K. Sethupathi and S. Ramaprabhu, *Int. J. Hydrogen Energy*, 37 (2012) 412.
9. J.F. Lin, V. Kamavaram and A.M. Kannan, *J. Power Sources*, 195 (2010) 466.
10. N. Alexeyeva, K. Tammeveski, A. Lopez-Cudero, J. Solla-Gullón and J.M. Feliu, *Electrochim. Acta*, 55 (2010) 794.
11. R. Jasinski, *Nature*, 201 (1964) 1212.
12. S. Baranton, C. Coutanceau, C. Roux, F. Hahn and J.-M. Léger, *J. Electroanal. Chem.* 577 (2005) 223.
13. E. Claude, T. Addou, J.-M. Latour and P. Aldebert, *J. Appl. Electrochem.* 28 (1997) 57.
14. G. Lalande, G. Faubert, R. Côté, D. Guay, J.P. Dodelet, L.T. Weng and P. Bertrand, *J. Power Sources*, 61 (1996) 227.
15. X. Li, B.N. Popov, T. Kawahara and H. Yanagi, *J. Power Sources*, 196 (2011) 1717.
16. H. Kavelage, A. Mecklenburg, U. Kunz and U. Hoffmann, *Chem. Eng. Technol.*, 23 (2000) 803.
17. V. Bambagioni, C. Bianchini, J. Filippi, A. Lavacchi, W. Oberhauser, A. Marchionni, S. Moneti, F. Vizza, R. Psaro, V. Dal Santo, A. Gallo, S. Recchia and L. Sordelli, *J. Power Sources*, 196 (2011) 2519.
18. Y. Yuan, J. Ahmed and S. Kim, *J. Power Sources*, 196 (2011) 1103.
19. Y. Nabe, S. Moriya, K. Matsubayashi, S.M. Lyth, M. Malon, L. Wu, N.M. Islam, Y. Koshigoe, S. Kuroki, M. Kakimoto, S. Miyata and J. Ozaki, *Carbon*, 48 (2010) 2613.
20. L. Ding, X. Dai, R. Lin, H. Wang and J. Qiao, *J. Electrochem. Soc.*, 159 (2012) F577.

21. I. Kruusenberg, L. Matisen, Q. Shah, A.M. Kannan and K. Tammeveski, *Int. J. Hydrogen Energy*, 37 (2012) 4406.
22. S.A. Mamuru and K.I. Ozoemena, *Electroanalysis*, 22 (2010) 985.
23. W. Zhang, A.U. Shaikh, E.Y. Tsui and T.M. Swager, *Chem. Mater.*, 21 (2009) 3234.
24. X. Deng, D. Zhang, X. Wang, X. Yuan and Z. Ma, *Chin. J. Catal.*, 29 (2008) 519.
25. T. Schilling, A. Okunola, J. Masa, W. Schuhmann and M. Bron, *Electrochim. Acta*, 55 (2010) 7597.
26. A. Okunola, B. Kowalewska, M. Bron, P.J. Kulesza and W. Schuhmann, *Electrochim. Acta*, 54 (2009) 1954.
27. Z. Xu, H. Li, G. Cao, Q. Zhang, K. Li and X. Zhao, *J. Mol. Catal. A: Chem.*, 335 (2011) 89.
28. A. Morozan, S. Campidelli, A. Filoramo, B. Jousselme and S. Palacin, *Carbon*, 49 (2011) 4839.
29. S.K. Kim and S. Jeon, *Electrochem. Commun.*, 22 (2012) 141.
30. P. Bogdanoff, I. Herrmann, M. Hilgendorff, I. Dorbandt, S. Fiechter and H. Tributsch, *J. New Mater. Electrochem. Systems*, 7 (2004) 85.
31. M. Lefevre, J.-P. Dodelet and P. Bertrand, *J. Phys. Chem. B.*, 106 (2002) 8705.
32. A. Widelöv and R. Larson, *Electrochim. Acta*, 37 (1992) 187.
33. I. Kruusenberg, N. Alexeyeva, K. Tammeveski, J. Kozlova, L. Matisen, V. Sammelselg, J. Solla-Gullón and J.M. Feliu, *Carbon*, 49 (2011) 4031.
34. A.T. Masheter, L. Xiao, G.G. Wildgoose, A. Crossley, J.H. Jones and R.G. Compton, *J. Mater. Chem.*, 17 (2007) 3515.
35. P. Gouerec, M. Savy and J. Riga, *Electrochim. Acta*, 43 (1998) 743.
36. M. Ladouceur, G. Lalande, D. Guay, J.P. Dodelet, L. Dignard-Bailey, M.L. Trudeau and R. Schulz, *J. Electrochem. Soc.*, 140 (1993) 1974.
37. M.C.M. Alves, J.P. Dodelet, D. Guay, M. Ladouceur and G. Tourillon, *J. Phys. Chem.*, 96 (1992) 10898.
38. A.J. Bard and L.R. Faulkner, *Electrochemical methods*. 2nd ed. New York: Wiley; 2001.
39. S. Gottesfeld, I.D. Raistrick and S. Srinivasan, *J. Electrochem. Soc.*, 134 (1987) 1455.
40. A. Morozan, S. Campidelli, A. Filoramo, B. Jousselme and S. Palacin, *Carbon*, 49 (2011) 4839.
41. R. Yamazaki, Y. Yamada, T. Ioroi, N. Fujiwara, Z. Siroma and K. Yasuda, *J. Electroanal. Chem.*, 576 (2005) 253.
42. Z. Mo, S. Liao, Y. Zheng and Z. Fu, *Carbon*, 50 (2012) 2620.
43. S. Gupta, D. Tryk, I. Bae, W. Aldred and E. Yeager, *J. Appl. Electrochem.*, 19 (1989) 19.
44. U.I. Kramm, I. Abs-Wurmbach, I. Herrmann-Geppert, J. Radnik, S. Fiechter and P. Bogdanoff, *J. Electrochem. Soc.*, 158 (2011) B69.
45. J.A.R. v. Veen, H.A. Coljin and J.F. v. Baar, *Electrochim. Acta*, 33 (1988) 801.
46. J.-P. Dodelet, in *N₄-Macrocyclic Metal Complexes*, 1st ed., J.H. Zagal, F. Bedioui and J.-P. Dodelet, Editors, Springer, New York (2006).
47. K. Wiesener, *Electrochim. Acta*, 31 (1986) 1073.
48. P.H. Matter, E.J. Biddinger and U.S. Ozkan, *Catalysis*, 20 (2007) 338.
49. J. Herranz, M. Lefevre, N. Larouche, B. Stansfield and J.-P. Dodelet, *J. Phys. Chem. C*, 111 (2007) 19033.
50. G. Lalande, R. Cote, D. Guay, J.-P. Dodelet, L.T. Weng and P. Bertrand, *Electrochim. Acta*, 42 (1997) 1379.
51. L. Elbaz, E. Korin, L. Soifer and A. Bettelheim, *J. Phys. Chem. Lett.*, 1 (2010) 398.
52. J. Zagal, S. Griveau, K.I. Ozoemena, T. Nyokong and F. Bedioui, *J. Nanosci. Nanotechnol.*, 9 (2009) 2201.